

DE • E • I G B A D I I ED  
A XI A I •

G BEY IN\* AND ANDBE G\*\*

A R | us n r G uss n qu r tur s or po

Using approximations of functions via exponentials instead of polynomials have been considered in e.g., [7, 12, 26] and, recently, in e.g., [17, 18, 13, 20, 21], where in [13, 20, 21] authors use band-limited exponentials with complex-valued exponents. In these papers the nodes are chosen to be equally spaced and, thus, such methods may be viewed as band-limited analogues of multistep schemes. As explained below, our method, dubbed Band-limited Collocation Implicit Runge-Kutta (BLC-IRK), uses unequally spaced nodes and is different from the earlier approaches as in e.g., [1, 8].

It is well-known that choosing between equally spaced and unequally spaced nodes on a specified time interval results in significantly different properties of ODE solvers. For example, polynomial-based multistep schemes have  $\{\operatorname{Re}(z) \leq 0, z \in \mathbb{C}\}$  as the region of absolute stability (A-stable) only if their order does not exceed 2, the so-called Dahlquist barrier. In contrast, an A-stable implicit Runge-Kutta (IRK) scheme may be of arbitrary order. A class of A-stable IRK schemes uses the Gauss-Legendre quadrature nodes on each time interval and the order of such methods is  $2s$ , where  $s$  is the number of nodes (see, e.g., [16]). A-stability assures that growth and decay of numerical solutions ex-

In this paper we demonstrate that, within IRK collocation methods, quadratures based on polynomials may be replaced by quadratures for band-limited exponentials. The nodes of these quadratures do not accumulate significantly toward the end points of an interval (a heuristic reason for an improved arrangement of nodes is that the exponentials do not grow anywhere within the interval). Our method addresses numerical integration of ODEs whose solutions are well approximated by band-limited exponentials. We note that band-limited exponentials have been successfully used in problems of wave propagation [3] (see also [29, 20]), where it is natural to approximate solutions by band-limited functions.

Unlike the classical Gaussian quadratures for polynomials that integrate exactly a subspace of polynomials up to a fixed degree, the Gaussian type quadratures for exponentials use a finite set of nodes to integrate an infinite set of functions, namely,  $e^{ibx}$   $|b| \leq c$  on the interval  $|x| \leq 1$ . As there is no way to accomplish this exactly, these quadratures are constructed so that all exponentials with  $|b| \leq c$  are integrated with accuracy of at least  $\epsilon$ , where  $\epsilon$  is arbitrarily small but finite. Such quadratures were constructed in [2] and, via a different approach in [36] (see also [28]). As observed in [3], quadrature nodes of this type do not concentrate excessively toward the end of the interval. The density of nodes increases toward the end points of the interval only by a factor that depends on the desired accuracy but

qdr11.277(c)3.38586(o)-2ur.



in many cases leads to significant improvement in performance of algorithms for interpolation, estimation and solving partial differential equations [3, 29, 20].

**2.2. Band-limited functions** It is well-known that a function whose Fourier Transform has compact support can not have compact support itself unless it is identically zero. On the other hand, in physics duration of all signals is finite and their frequency response for all practical purposes is also band-limited. Thus, it is important to identify classes of functions which are essentially time and frequency limited. Towards this end, it is natural to analyze an operator whose effect on a function is to truncate it both in the original and the Fourier domains. Indeed, this has been the topic of a series of seminal papers by Slepian, Landau and Pollak, [35, 22, 23, 31, 32, 33, 34], where they observed (inter alia) that the eigenfunctions of such operator (see (2.2) below) are the Prolate Spheroidal Wave Functions (PSWFs) of classical Mathematical Physics.

While periodic band-limited functions may be expanded into Fourier series, neither the Fourier series nor the Fourier integral may be used efficiently for non-periodic functions on intervals. This motivates us to consider a class of functions (not necessarily periodic) admitting a representation via exponentials  $e^{ibx}$ ,  $|b| \leq c$ ,  $x \in [-1, 1]$ , with a fixed parameter  $c$  (bandlimit). Following [2], let us consider the linear space of functions

$$E_c = \{ u \in L^\infty([-1, 1]) \mid u(x) = \sum_{k \in \mathbb{Z}} a_k e^{ib_k x} : \{a_k\}_{k \in \mathbb{Z}} \in \ell^1, b_k \in [-1, 1] \}.$$

Given a finite

3geofG211.9552Tf952d[(G[(u)-5.09921]TJR2011.9552TfTd[(i)-1.125221)4.03117]TJR387(c)3.38994(e)3.3uxs(e)3

where the number of nodes  $M = c/\epsilon + O(\log c)$  is near  $y^{\text{opt}}$  a  
the nodes and we sets a natural hierarchy  $k = 1, \dots, M-k+1$   
and  $w_k = w_{M-k+1}$

Remark 2 The construction in [2] is more general and yields quadra-

similar to orthogonal polynomials; they are orthonormal, constitute a Chebychev system, and admit a version of Gaussian quadratures [36].

Since the space  $E_c$  is dense in  $B_c$  (and vice versa) [2], we note that the quadratures in [36] may potentially be used for the purposes of this paper as well (the nodes of the quadratures in [36] and those used in this paper are close but are not identical). Importantly, given accuracy  $\epsilon$ , the functions  $\phi_0^c, \phi_1^c, \phi_2^c, \dots, \phi_{M-1}^c$  may be used as a basis for interpolation on the interval  $[-1, 1]$  with  $x_1, x_2, \dots, x_M$  as the interpolation nodes, provided that these are quadrature nodes constructed for the bandlimit  $2c$  and accuracy  $\epsilon^2$ . Given functions  $\phi_0^c, \phi_1^c, \phi_2^c, \dots, \phi_{M-1}^c$ , we can construct an analogue of the Lagrange interpolating polynomials,  $R_k^c(x) = \sum_{j=0}^{M-1} k_{kj} \phi_j^c(x)$ ,  $x \in [-1, 1]$ , by solving

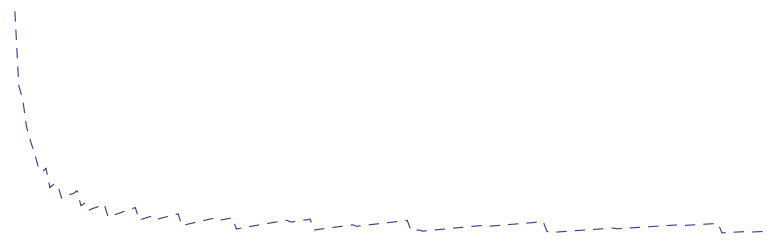
$$(2.6) \quad k_{kl} = R_k^c(x_l) = \sum_{j=0}^{M-1} k_{kj} \phi_j^c(x_l)$$

for the coefficients  $k_{kj}$ . The matrix  $\phi_j^c(x_l)$  in (2.6) is well conditioned.

A well-known problem associated with the numerical use of orthogonal polynomials is concentration of their roots near the ends of the interval. Let us consider the ratio

$$(2.7) \quad r(M, \epsilon) = \frac{2^{-M} - 1}{\lfloor M/2 \rfloor - \lfloor M/2 \rfloor - 1},$$

where  $\epsilon = M/2$





Following [2], we discretize (2.2) using nodes  $\{m\}_{m=1}^M$  and weights  $\{w_m\}_{m=1}^M$  and obtain an algebraic eigenvalue problem,

$$(2.8) \quad \sum_{l=1}^M w_l e^{ic_l} j_l(x) = \lambda_j j_l(x).$$

The approximate PSWFs on  $[-1, 1]$  are then defined consistent with (2.2) as

$$(2.9) \quad j_j(x) = \frac{1}{j} \sum_{l=1}^M w_l e^{ic_l} j_l(x),$$

where  $\lambda_j$  are the eigenvalues and  $j_l(x)$  the eigenvectors in (2.8). Following [2], we then define the interpolating basis for band-limited functions as

$$(2.10) \quad R_k(x) = \sum_{l=1}^M r_{kl}$$

where  $\{t_j\}_{j=1}^M$  are Gaussian nodes for band-limited exponentials on  $[0, 1]$  (constructed for an appropriate bandlimit  $c$  and accuracy  $\epsilon$ ). We approximate

$$(3.2) \quad \tilde{f}(t, (t)) - \sum_{j=1}^M \tilde{f}(t_j, (t_j)) R_j(t) \quad , \quad [0, 1]$$

where  $R_j(t)$  are interpolating basis functions associated with these quadratures and briefly described in Section 2.3 (see [2, 3] for details). Using (3.2), we replace  $\tilde{f}$  in (3.1) and evaluate  $\tilde{f}(t)$  at the quadrature nodes yield2

so that the integral equation (3.1) may be written as

$$(3.5) \quad (t) = e^{tL}$$

or

$$\int_{-1}^1 R_j(s) ds - R_k(\xi) = w_k \int_{-1}^1 R_j(s) ds < \epsilon^2,$$

and

$$(3.9) \quad \int_{-1}^1 R_k(\xi) d\xi - \sum_{l=1}^M w_l R_k(\xi_l) < \epsilon^2,$$

or

$$\int_{-1}^1 R_k(s) ds - w_k < \epsilon^2.$$

*Proof* The relations in (3.8) and (3.9) is the property of the quadrature, since the bandlimit of the product  $F_j(\xi)F'_k(\xi)$  is less or equal to  $2c$  and that of  $R_k(\xi)$  is less or equal to  $c$ . Due to the interpolating property of  $R_k(\xi)$ , we have

$$(3.10) \quad \sum_{l=1}^M w_l F_j(\xi_l) F'_k(\xi_l) = \sum_{l=1}^M \int_{-1}^1 R_j(s) ds - w_l R_k(\xi_l) = w_k \int_{-1}^1 R_j(s) ds$$

and

$$\sum_{l=1}^M w_l R_k(\xi_l) = w_k$$

Also, by definition,

$$\int_{-1}^1 F_j(\xi) F'_k(\xi) d\xi = \int_{-1}^1 R_j(s) ds - R_k(\xi),$$

and the result follows.  $\square$

or Let  $\{\xi_j\}_{j=1}^M$  be quadrature nodes of the quadrature for the band  $t \leq 2c$  and accuracy  $\epsilon^2$  and  $R_k(\xi) = \sum_{j=1}^M R_{kj}(\xi)$ ,  $k, j = 1, \dots, M$  the correspond nodes. Let us define weights for the quadrature as

$$(3.11) \quad w_k = \int_{-1}^1 R_k(\xi) d\xi$$

and the node  $\xi_k$  at  $x$  as

$$(3.12) \quad S_{kj} = \frac{\int_{-1}^1 R_j(s) ds - R_k(\xi_j)}{w_k}, \quad k, j = 1, \dots, M.$$

then

$$(3.13) \quad w_k S_{kj} + w_j S_{jk} - w_k w_j = 0,$$

and the proof is complete using these nodes and weights satisfy property

*Proof* Using Proposition 4, we observe that the weights defined in (3.11) are the same (up to accuracy  $\epsilon^2$ ) as those of the quadrature. The result follows by setting  $F_k(\cdot) = \int_{-1}^{\cdot} R_k(\cdot) d$ ,  $F_k'(\cdot) = R_k(\cdot)$  and integrating by parts to obtain

$$\begin{aligned} w_k S_{kj} + w_j S_{jk} - w_k w_j &= \int_{-1}^1 F_j(\cdot) F_k'(\cdot) d + \int_{-1}^1 F_k(\cdot) F_j'(\cdot) d - w_k w_j \\ &= F_j(1) F_k(1) - w_k w_j. \end{aligned}$$

By the definition of the weights, we have  $F_k(1) = w_k$  and, hence,  $F_j(1) F_k(1) - w_k w_j = 0$ .  $\square$

3.4. Construction of test problem. There are at least three approaches to compute the integration matrix. Two of them, presented in the Appendix, rely on Theorem 5 and differ in the construction of interpolating basis functions. In what appears to be a simpler approach, the integration matrix may also be obtained without computing interpolating basis functions explicitly and, instead, using a collocation condition derived below together with the symplectic condition (3.13).

We require that our method accurately solves the test problems

$$y' = ic_m y, \quad y(-1) = e^{-ic_m}, \quad m = 1, \dots, M,$$

on the interval  $[-1, 1]$ , where  $c_m$  are the nodes of the quadrature. Specifically, given solutions of these test problems,  $y_m(t) = e^{ic_m t}$ , we require that (3.3) holds at the nodes  $t = c_k$  with accuracy  $\epsilon$ ,

$$(3.14) \quad e^{ic_m c_k} - e^{-ic_m c_k}$$

Using (3.16) and casting (3.14) as an equality, we obtain equations for the matrix entries  $A_{kj}$

3.5. As shown in e.g. [16, Section 4.3], in order to ascertain stability of an IRK method, it is sufficient to consider the rational function

$$(3.19) \quad r(z) = 1 + z^t (I - zS)^{-1},$$

where  $S$  is the integration matrix,  $\mathbf{b}$  is a vector of weights and  $\mathbf{c}$  is a vector with all entries set to 1, and verify that  $|r(z)| \leq 1$  in the left half of the complex plane,  $\text{Re}(z) \leq 0$ . This function is an approximation of the solution  $e^{zt}$  at  $t = 1$  of the test problem

$$y' = zy, \quad y(0) = 1$$

computed via (3.3) and (3.4) on the interval  $[0, 1]$ . If all poles of  $r(z)$  have a positive real part, then it is sufficient to verify this inequality only on the imaginary axis,  $z = iy, y \in \mathbb{R}$ . In fact, it may be possible to show that  $r(z)$  is unimodular on imaginary axis,  $|r(iy)| = 1$ , for  $y \in \mathbb{R}$ . Implicit Runge-Kutta methods based on Gauss-Legendre nodes are A-stable (see e.g [16]) and, indeed, for these methods  $r(z)$  is unimodular on imaginary axis.

Given an  $M \times M$  matrix  $S$  with  $M_1$  complex eigenvalues and  $M_2$  real eigenvalues implies that the function  $r(z)$  in (3.19) has  $2M_1 + M_2 = M$  poles. If this function is unimodular on the imaginary axis then it is easy to show that it has a particular form,

$$(3.20) \quad r(z) = \prod_{k=1}^{M_1} \frac{z + \frac{-1}{k}}{z - \frac{-1}{k}} \prod_{k'=1}^{M_2} \frac{z + \frac{-1}{k'}}{z - \frac{-1}{k'}}.$$

Currently, we do not have an analytic proof of A-stability of BLC-IRK method; instead we verify (3.20) numerically. We compute eigenvalues of the integration matrix to obtain the poles of  $r(z)$  and check that all eigenvalues have a positive real part separated from zero. For example, the integration matrix for the BLC-IRK method with 64 nodes (bandlimit  $c = 17$ ) has all eigenvalues with real part larger than  $0.7 \cdot 10^{-3}$  (see Figure 3.1). One way to check that  $r(z)$  has the form (3.20) is to compute  $r(-\frac{-1}{k})$  for complex valued and  $r(-\frac{-1}{k})$  for real valued eigenvalues in order to observe if these are its zeros. In fact, it is the case with high (quadruple) precision.

One can argue heuristically that since a rational function with  $M$  poles has at most  $2M$  real parameters (since matrix  $S$  is real its eigenvalues appear in complex conjugate pairs) and since, by construction,  $r(iy)$  for  $|y| \leq c$  is an accurate approximation to  $e^{iy}$  (which is obviously unimodular),  $r(z)$  is then unimodular. It remains to show it rigorously; a possible proof may depend on demonstrating a conjecture in Remark 6.

- 
- 
- 
- 
- 
- 
- 
-



Thus, the only constraint on the size of the interval is the requirement that the (standard) fixed point iteration for (3.6) converges .

Let  $N_{it}$  denote the number of iterations, which can either be set to a fixed number or be determined adaptively. Labeling the intermediate solutions in the iteration scheme as  $y^{(n)}$ ,  $n = 1, \dots, N_{it}$ , we have

(1) Initialize  $y^{(1)}(t_m) = 0$ ,  $m = 1, \dots, M$ .

(2) For  $n = 1, \dots, N_{it}$   
 For  $k = 1, \dots, M$

(a) Update the solution at the node  $k$ :

$$y^{(n)}(t_k) = e^{t_k L} y_0 + \int_0^{t_k} S_{kj} e^{t(k-j)L} f_j(t_j, y^{(n)}(t_j)) dt_j$$

(b) Update the right hand side at the node  $k$ :  $f_k(t_k, y^{(n)}(t_k))$

We note that the updated value of  $y^{(n)}(t_k)$  is used in the computation at the next node  $k+1$  within the same iteration  $n$ . This modification of the standard fixed point iteration is essential for a faster conver

gravitational model,  $\mu$  is the Earth's gravitational constant and  $R$  is chosen to be the Earth's equatorial radius. Choosing the Cartesian coordinates, we write  $V^{(N)}(r)$ ,  $r = (x, y, z)$ , assuming that the values  $V^{(N)}(r)$  are evaluated via (4.1) by changing from the Cartesian to the spherical coordinates,  $r = \sqrt{x^2 + y^2 + z^2}$ ,  $\theta = \arcsin(z/r)$  and  $\phi = \arctan(y/x)$ .

We formulate the system of ODEs in the Cartesian coordinates and denote the solution as  $r(t) = (x(t), y(t), z(t))$ . Setting  $G^{(N)}(r) = -\nabla V^{(N)}(r)$ , we consider the initial value problem

(4.3)

$$\frac{d^2}{dt^2}r(t) = -G^{(N)}(r(t)), \quad r(0) = r_0 = \begin{pmatrix} x_0 \\ y_0 \\ z_0 \end{pmatrix}, \quad r'(0) = v_0 = \begin{pmatrix} x'_0 \\ y'_0 \\ z'_0 \end{pmatrix}.$$

We observe that the first few terms of the Earth's gravitational models are large in comparison with the rest of the model terms. For example, in EGM96 [25], the only non-zero coefficients for  $Y_2(\theta, \phi)$  are  $\bar{C}_{20}$ ,  $\bar{C}_{22}$  and  $\bar{S}_{22}$ .

Next, let us write the orbit determination problem in a form that conforms with the algorithm in Section 4.1. Effectively, we make use of the fact that system (4.3) is of the second order. We define the six component vector

$$\mathbf{u}(t) = \begin{bmatrix} \mathbf{r}(t) \\ \dot{\mathbf{r}}(t) \end{bmatrix}$$



We then compute weights using (3.11),

$$w_k = \int_{-1}^1 R_k^c(x) dx = \int_{j=0}^{M-1} \int_{-1}^1 c_j(x) dx = \int_{j=0}^{M-1} c_j(0).$$

Next we define

$$K_i^c(x) = \int_{-1}^x R_i^c(s) ds = \int_{j=0}^{M-1} \int_{-1}^x c_j(s) ds = \int_{j=0}^{M-1} c_j(x),$$

where

$$(6.2) \quad c_j(x) = \int_{-1}^x c_j(s) ds.$$

In order to compute the integrals...

ij

⓪Td (J)G5 ⓪Td (J)

) )

$$dx = \int_1^J c_j(x) \quad \text{⓪Td (J)G5 ⓪Td (J)}$$

*Proof* Integrating (6.3) by parts, we obtain

$$(6.9) \quad I_{jj'} + I_{j'j} = \int_{-1}^1 c_j(1) c_{j'}(1) - \int_{-1}^1 c_j(-1) c_{j'}(-1) = \int_{-1}^1 c_j c_{j'} - \int_{-1}^1 c_j c_{j'}$$

and, since  $c_j(0) = 0$  if  $j$  is odd (due to parity of PSWFs), we arrive at (6.5) and (6.6).

Using (6.2) and (6.1), we have

$$c_j(x) = \frac{1}{j} \int_{-1}^1 e^{icys} ds \int_{-1}^x c_j(y) dy = \frac{1}{j} \int_{-1}^1 \frac{e^{icyx} - e^{-icy}}{icy} c_j(y) dy,$$

and, thus,

$$(6.10) \quad \begin{aligned} I_{jj'} &= \frac{1}{j} \int_{-1}^1 \int_{-1}^1 \frac{e^{icyx} - e^{-icy}}{icy} c_j(y) dy c_{j'}(x) dx \\ &= \frac{j'}{ic} \int_{-1}^1 c_j(y) \frac{c_{j'}(y)}{y} dy - c_j(0) \int_{-1}^1 \frac{c_{j'}(y)}{y} e^{-icy} dy. \end{aligned}$$

It follows from (6.10) that if  $j$  is even and  $j'$  is odd (so that  $c_{j'}(0) = 0$ ), we obtain (6.7) and

$$I_{j'j} = \frac{j}{ic} \int_{-1}^1 c_j(y) \frac{c_{j'}(y)}{y} dy - c_j(0) \int_{-1}^1 \frac{c_{j'}(y)}{y} e^{-icy} dy.$$

Introducing

$$u(x) = \int_{-1}^1 \frac{c_{j'}(y)}{y} e^{-icyx} dy,$$

we have

$$u'(x) = -ic \int_{-1}^1 c_{j'}(y) e^{-icyx} dy = -ic \int_{-1}^1 c_{j'}(x)$$

so that

$$u(x) = u(a) - ic \int_a^x c_{j'}(s) ds.$$

Setting  $x = 1$  and  $a = 0$ , we obtain

$$\int_{-1}^1 \frac{c_{j'}(y)}{y} e^{-icy} dy$$

6.2. Computing the Fourier transform of  $f(x)$ .  
 If the interpolating basis for band-limited functions is defined via (2.10), then the coefficients  $r_{kl}$  are obtained using

$$(6.11) \quad r_{km} = R_k(c_m) = \sum_{l=1}^M r_{kl} e^{ic_l c_m}$$

by inverting the matrix  $E = \{e^{ic_l c_m}\}_{l,m=1,\dots,M}$ . We have

$$R_k(x) = \int_{-1}^1 R_k(s) ds = \sum_{l=1}^M r_{kl} \frac{e^{ic_l x} - e^{-ic_l x}}{ic_l}$$

and compute

$$\begin{aligned} w_k S_{kl} &= \int_{-1}^1 R_l(x) R_k(x) dx \\ &= \sum_{j,j'=1,\dots,M} r_{kj} r_{lj'} \int_{-1}^1 \frac{e^{ic_j x} - e^{-ic_j x}}{ic_j} \frac{e^{ic_{j'} x} - e^{-ic_{j'} x}}{ic_{j'}} dx \\ &= \sum_{j,j'=1,\dots,M} r_{kj} r_{lj'} G_{jj'} \end{aligned}$$

where

$$G_{jj'} = 2 \frac{\text{sinc}(c_j + c_{j'}) - e^{-ic_j c_{j'}} \text{sinc}(c_j)}{ic_{j'}}$$

Thus, we have

$$w_k S_{kl} = E^{-1} G E^{-1}_{kl}$$

R N

Journal of Computational and Applied Mathematics

Appl. Comput. Harmon. Anal.

Wave Motion

Journal of Scientific Computing

Bro n F J urr us o pon nt su n st p st p n  
t r ton **Mathematical Tables and Other Aids to Computation**

H v r Fr qu n v u ton or pon nt tt un utt  
nt o s **Journal of computational and applied mathematics**

D r n J G r w r **Stability of the Runge-Kutta methods for sti  
nonlinear di erential equations** Nort Ho n A st r m

D pt o D ns or G o t st mD ns pp n A n n  
port n r port D A

A Dutt Gr n r n o n p tr rr orr ton nt o s  
or or n r r nt qu tons **BIT**

G uts Nu mr nt r ton o or n r r nt qu tons s on  
tr ono mtr po no m s **Numerische Mathematik**

A G s r n o n A n w ss o ur t so v rs or or n r  
r nt qu tons **Journal of Scientific Computing**

D Gott n A rs **Numerical analysis of spectral methods: theory  
and applications** o t or In ustr n App t mt s

p CB N F on Con r n r s n App t  
mt s No

J Hu n J J n non A r tn t onv r n o sp tr  
rr orr ton nt o s **J. Comput. Phys.**

A Is r s **A first course in the numerical analysis of di erential equations**  
C mr n v rst r ss

G I ru G B r n H D r ts o t pon n  
t tt n mt st p ort n or rst or r DEs **Journal of computational  
and applied mathematics**

G I ru n n B G n H D r Fr qu n v u ton n po  
n nt tt n mt st p ort n or DEs **Journal of Computational and  
Applied Mathematics**

J J n J Hu n r ov rr orr ton r t mt o o n s  
tr nspos **Journal of Computational Physics**

Y on n o n A n w ss o ur t r nt ton  
s ms s ont pro t sp ro w v un tons **Appl. Comput. Har-  
mon. Anal.**

D us n r n o n A H A ur t ov r or t r n r D r  
nt Equ tons **SIAM Journal on Scientific Computing** A A

H J n u n H o ro t sp ro w v un tons Four r  
n ss n un rt nt II **Bell System Tech. J.**

H J n u n H o ro t sp ro w v un tons Four r  
n ss n un rt nt III **Bell System Tech. J.**

A ton n non I p tons o t o o qu r tur  
no s or r nt r rr orr tons nt o s or or n r r nt



